Supervised Feature-Based Classification of Multi-Channel SAR Images

D. Borghys, Y. Yvinec, C. Perneel,

Signal & Image Centre, Royal Military Academy, Renaissancelaan 30, B-1000 Brussels

A. Pizurica, W. Philips

Dept. of Telecomm. and Inf. Proc., Univ. of Ghent, St-Pietersnieuwsstraat 41, B-9000 Gent

Abstract

This paper describes a new method for a feature-based supervised classification of multi-channel SAR data. Classic feature selection and classification methods are inadequate due to the diverse statistical distributions of the input features. A method based on logistic regression (LR) and multinomial logistic regression (MNLR) for separating different classes is therefore proposed. Both methods, LR and MNLR, are less dependent on the statistical distribution of the input data. A new spatial regularization method is also introduced to increase consistency of the classification result. The classification method was applied to a project on humanitarian demining in which the relevant classes were defined by experts of a Mine Action Center. A ground survey mission collected learning and validation samples for each class. Results of the proposed classification methods are shown and compared to a maximum likelihood classifier.

Key words: SAR Image Classification, Logistic Regression, Multinomial Logistic Regression, Multi-Channel SAR

1 Introduction

This article presents a new method for supervised classification of multi-channel SAR data. The method was applied in a project on humanitarian demining. It was delivered as one of the tools that aim at helping a human

Email address: Dirk.Borghys@elec.rma.ac.be (D. Borghys).

operator to decide whether a region is potentially mined or not. Relevant land-cover classes were defined by the experts of a Mine Action Center. A set of multi-channel SAR data, including polarimetric and dual-pass interferometric data at different frequencies was acquired using the E-SAR system of the German Aerospace Center (DLR). The images from different bands (P, L , C and X-band) cover the same region but each band has a different spatial resolution. Geocoding information was also provided. A ground survey mission collected the necessary ground truth information for each of the defined classes.

For classification of polarimetric SAR (POLSAR) images, several unsupervised approaches have been proposed, based on various polarimetric decomposition methods (Cloude and Pottier , 1996). The most used method is the decomposition of Cloude and Pottier (Cloude and Pottier , 1997). In this method the polarimetric information is converted into three parameters (entropy H, α-angle and Anisotropy A) to which the authors have associated an elegant physical interpretation. They sub-divided the feature space formed by the three parameters into regions that correspond to distinct scattering behaviors. However, the exact borders of these different regions depend on many factors. Different methods were suggested to make these borders flexible. In Lee et al. (1999) the samples in the feature space, spanned by the three Cloude parameters, are regrouped based on the complex Wishart distribution. In Hellmann (2000) a supervised classification method based on neural networks and fuzzy logic is used to learn the class borders from the available learning samples. The advantage of the approach proposed in Hellmann (2000) is that other input features can be easily added in order to increase the discrimination ability of the classification. In Hellmann (2000) the largest eigenvalue (λ_1) of the polarimetric coherence matrix and the interferometric coherence ρ are added to the feature set. In Lee et al. (1999b) a supervised classification is proposed based on the complex Wishart distribution of the polarimetric covariance matrix. This method is regarded as the recommended method for supervised classification of polarimetric SAR data (Rodriguez et al., 2003). The method can also be used for multi-frequency SAR data. However, it requires a one-to-one correspondence on pixel-level between the single-look complex (SLC) data of all the used channels and it does not allow to combine the covariance data with other types of features such as textural features or backscattered intensity. Alberga (2004) showed that the approach based on the covariance matrix does provide important information about the scatterers on the ground, but that extra information (e.g. backscatter amplitude or texture) can be needed in order to distinguish complex classes.

This led us to the idea to develop an approach that allows to take into account a set of input features with diverse statistical properties, representing for instance radiometric, polarimetric and polarimetric information. The developed approach combines feature selection with the combination of the features into a classification function. We already developed (Borghys et al., 2004) an ap-

proach based on logistic regression, which considers each class separately and tries to distinguish it from all others by combining the input features into a non-linear function, the logistic function. The method allows us to add features easily. Moreover, for each class a "detection image", with a well-defined statistical meaning, is obtained. The value at each pixel in the detection image represents the conditional probability that the pixel belongs to that class, given all input features. The logistic regression implicitly performs a feature selection. In order to improve the developed method, in this paper we replaced logistic regression by multinomial logistic regression (MNLR). MNLR gives better results due to the fact that it takes into account constraints between all classes involved in the classification. In Borghys et al. (2004b) we introduced a hierarchy in the classification: classes that are easily distinguished are detected first and sub-sequent steps of the classification only consider remaining classes. The current paper describes in more detail the approach presented in the workshop paper (Borghys et al. , 2004b). Furthermore, the spatial regularization method is improved and the different proposed classification methods are compared among them and to a classical maximum likelihood classifier.

2 Input Data

2.1 Overview of the SAR data set

The method was applied to a project on humanitarian demining (the "SMART" project) for which SAR data at 4 different frequencies were acquired. P-band and L-band are full-polarimetric, dual-pass interferometric. For C- and X-band only VV-polarisation was acquired. All data were delivered as Single-Look Complex (SLC) data as well as geocoded amplitude data. The pixel spacing in the SLC data of different bands is not the same. Together with the data, we therefore also received geocoding matrices that enable us to extract polarimetric and interferometric information using the SLC data and geocode the results afterward. Table 1 presents principal characteristics of the SAR data.

Band	Wavelength	Polarisation	Size in pixels $[W \times H]$	Pixel Spacing $[Range \times Azimuth]$
P	70 cm	HH,HV,VV	1410×5790	$1.50m \times 0.70m$
L	23 cm	HH,HV,VV	1452×9598	$1.50m \times 0.43m$
C	5.6 cm	VV	1456×11350	$1.50m \times 0.36m$
X	3 cm	VV	1455×11753	$1.50m \times 0.35m$

Table 1
Overview of the principal characteristics of the image set

2.2 Derived feature set

From the input SAR data, several input features were derived:

- Radiometric information: values in the speckle reduced log-intensity images of each frequency and each polarisation (8 features). The speckle reduction method (Pizurica et al. , 2001) combines a context-based, locally adaptive, wavelet shrinkage and Markov Random Fields to limit blurring of edges, by incorporating prior knowledge about possible edge configurations.
- Polarimetric information: provided by the parameters of the Cloude decomposition (Cloude and Pottier , 1997) (H, α -angle and λ_1). λ_1 is the largest eigenvalue of the polarimetric coherence matrix. These parameters are available in P- and L-band, resulting in 6 features.
- Interferometric information: From the pairs of dual-pass interferometric images, the interferometric coherence (ρ) is calculated for HH-polarisation. This results in 2 features (ρ_L and ρ_P)
- Spatial information: Some basic spatial information is included in the feature list. It consists of the results of a bright and a dark line detector (Borghys et al. , 2003). The line detector uses a multi-variate statistical test for detecting line structures and is applied on the 8 speckle reduced, geocoded, log-intensity images. These input channels are treated by the detector as a single vectorial input and a single result is obtained for the dark lines and another one for the bright lines (2 features).

The polarimetric and interferometric features were determined on the slant-range SLC SAR data and then geocoded. The speckle reduction was applied on the geocoded images. In total, 18 input features are available.

2.3 Ground truth

A field survey mission was organized to acquire ground truth, i.e. the relevant classes of land-cover in the scene were determined and for each of them, examples were given. The ground truth objects were then divided into a learning set and a validation set. Both sets contain around 200 objects (regions) from the test-site. The learning set is used for the optimization of the parameters of the supervised classification. For the SMART project data were acquired over three areas in Croatia. Each area has distinct vegetation types. In the current paper the test-site with the largest diversity of land-cover types - a fertile plain near a river with intensive agricultural activity - was chosen for validation of the proposed methods. Table 2 shows the classes used for the learning set for this test-site. For the validation set, some classes are merged because their distinction does not give relevant information to the deminers. The different

C1:	Abandoned Land	C5:	Fields of Corn	C9:	Radar Shadows
C2:	Roads	C6:	Fields Without Veg.	C10:	Water
C3:	Fields of Barley	C7:	Forests & Hedges	C11:	Residential Areas
C4:	Fields of Wheat	C8:	Pastures		

Table 2
Classes used in the learning set

types of crops (C3, C4 and C5) are merged into a class "Fields in use with vegetation". They are kept separate for the learning to avoid complicating the classification task by having heterogeneous classes.

3 Statistical Methods

The classification scheme uses two statistical methods: logistic regression and multinomial logistic regression. Both methods offer a way to combine the different input features while at the same time performing a feature selection.

3.1 Logistic Regression

Logistic regression (Hosmer , 2000) (LR) is developed for dichotomous problems where a target class has to be distinguished from the background. The method combines the input parameters into a non-linear function, the logistic function, defined as:

$$p_{x,y}\left(target \mid \overrightarrow{F}\right) = \frac{exp\left[\beta_o + \sum_i F_i(x,y)\beta_i\right]}{1 + exp\left[\beta_o + \sum_i F_i(x,y)\beta_i\right]}. \quad (1)$$

$p_{x,y}\left(target \mid \overrightarrow{F}\right)$ is the conditional probability that a pixel (x,y) belongs to the considered class (target class) given the vector of input features ($\overrightarrow{F}$) at the given pixel. $\overrightarrow{F}$ is the vector of features calculated at each pixel, $F_i(x,y)$ is the value of the i^{th} feature in pixel (x,y). The logistic regression (i.e. the search for the $\beta_i's$) was carried out using Wald's forward step-wise method. In this method, at each step, the most discriminant feature is added and the significance of adding it to the model is verified. This means that not all features will necessarily be included into the model. The logistic regression thus gives an optimal combination of a sub-set of input parameters and also provides an objective method for determining the impact of adding each parameter to the model on the classification. Applying the obtained combination to the

complete image set, a new image - a "detection image" - is obtained, in which the target class under consideration is bright and the background dark.

3.2 Multinomial Logistic Regression

Multinomial logistic regression (Hosmer , 2000) (MNLR) is a generalization of logistic regression to multiple classes. In the multinomial logistic regression all classes are considered at the same time. The last class is the so-called baseline class (j^*). This time a set of combinations is found such that

$$p_{x,y}\left(Class_j \mid \overrightarrow{F}\right) = \frac{exp\left[\beta_{o,j} + \sum_i F_i(x,y)\beta_{i,j}\right]}{1 + \sum_{k \neq j^*} exp\left[\beta_{0,k} + \sum_i F_i(x,y)\beta_{i,k}\right]}, \tag{2}$$

for the non-baseline classes, where the sum in the denominator is over all classes, except the baseline class, and

$$p_{x,y}\left(Class_{j^*} \mid \overrightarrow{F}\right) = \frac{1}{1 + \sum_{k \neq j^*} exp\left[\beta_{0,k} + \sum_i F_i(x,y)\beta_{i,k}\right]}, \tag{3}$$

for the baseline class. In MNLR the statistical significance of each feature in the classification is given. Features with low significance are removed from the set of input features and the MNLR is re-run.

4 Derived Supervised Image Classification Methods

For each class of interest, examples are extracted from the learning set. Typically 800 pixels are randomly selected for each class of the learning set. The values of the input features calculated in these pixels are used to find the logistic or multinomial logistic function's parameters (the β_i or $\beta_{i,j}$ in equations 1 to 3). The search for these parameters requires the use of complex optimization methods. We used the commercial package SPSS for finding these parameters.

4.1 Classification based on LR and MNLR

The actual classification applies the LR and MNLR functions, with the parameters found in the learning set, to the features calculated on the complete scene. Both LR and MNLR thus give detection images per class corresponding to the conditional probability that the pixel belongs to the class, given all

input features. The classification image is obtained by assigning to each pixel the class for which the conditional probability is maximal.

4.2 Hierarchical Classification Method (HM)

In SAR images, some classes are more easy to detect than others. An hierarchical method was developed in order to take advantage of this fact. Classes that are easily distinguished are detected first. Sub-sequent steps of the classification only consider remaining classes. This means that the full discriminative power of the input features is used to solve a sub-problem of the classification at each level of the classification tree. Fig. 1 presents an overview of the classification tree used in this project. At the first level logistic regression (LR) is used to separate the class "Forests and Hedges" from all other classes. For separating the other classes, MNLR is used. In the second level classes that are difficult to distinguish (e.g. water, roads and radar shadow) are grouped. These are separated in the third level of the tree.

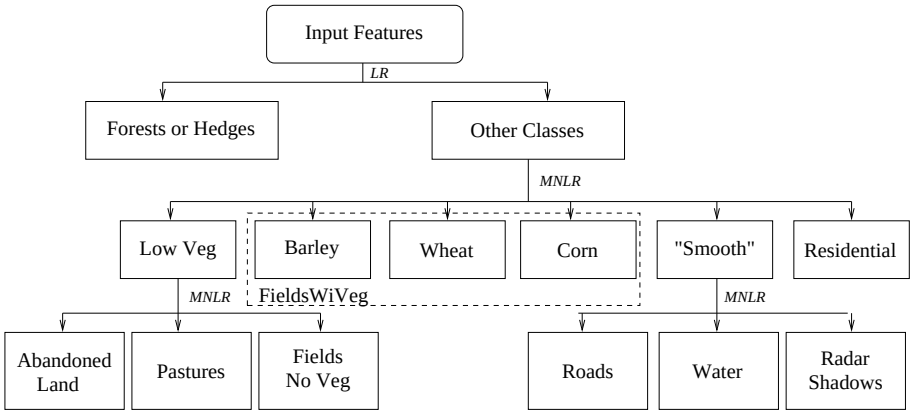

Figure 1. Overview of classification tree.

4.3 Spatial Regularization

When classes are similar, their distributions overlap and individual pixels can be miss-classified in "neighboring classes". In order to improve the results, spatial consistency is taken into account. In Borghys et al. (2004) and Borghys et al. (2004b) we used majority voting for spatial regularization (MVR), i.e. in a neighborhood (typically 3×3) of each pixel the sum of the conditional probability for each class is determined and the pixel is assigned to the class corresponding to the highest sum. In this paper we introduce an improved regularization method. The method, which replaces the MVR, is based on the "second best class" regularization (SBR). When classes are confused, the

values in the detection images (i.e. the conditional probabilities) are close to each other. In miss-classified pixels, the correct class often corresponds to the second highest value in the detection image. We therefore limit the majority voting to choose between either the current class or the "second best class". This avoids blurring of linear objects such as roads by the regularization: the regularization will only exchange roads for classes that are statistically similar (radar shadows and water). This method also allows larger windows for the regularization (we use 10×10).

5 Results and Discussion

Figure 2 shows the results of the method: (A) shows the polarimetric L-band E-SAR image after speckle reduction of the part of the test site (1.3km $\times$ 1.5 km). Examples of the main land-cover classes are indicated. In (B), as an example, the detection image for the class "Abandoned Land" is shown. (C) presents the classification result obtained by the hierarchical method (HM) without spatial regularization. (D) shows the HM results after SBR regularization.

The figure shows that the main structure of the land-cover is correctly identified by the classification. The regularization significantly reduces isolated miss-classified pixels. Some false alarms of residential areas are seen in the forests. This is in particular the case at the location of clearings in the forest. The SAR look direction was from right to left in the image. This explains the location of the radar shadows. The SAR imaging geometry is also responsible for the fact that most of the river is classified as shadow, because the river is bordered by trees. The two regions at the top left of the figure indicated by "FieldsNoVeg"(C6) show a typical example of the confusion between classes by the classifier: both instances of the class "FieldsNoVeg" were classified as "Pastures" (cf. pictures C and D). Picture B shows that the detection images could be used to get a fast overview of the location of a given class of interest. In particular, the class that is shown (abandoned agricultural land) is of great interest to the demining experts as it was defined by them as a possible indicator of the presence of minefields.

In order to obtain a more quantitative assessment of results, the validation set was used to determine a confusion matrix for the different classification methods. Table 3 shows the confusion matrix for the hierarchical method with the SBR regularization. From this matrix two statistics are calculated for the validation: the Producer's Accuracy (PA) and the User's Accuracy (UA). PA is the number of pixels correctly classified as a given class to the total number that actually belongs to that class. PA is thus related to the probability of detection. UA is the ratio of the number of pixels correctly classified as a given class to the total number of pixels classified as that class. UA is related

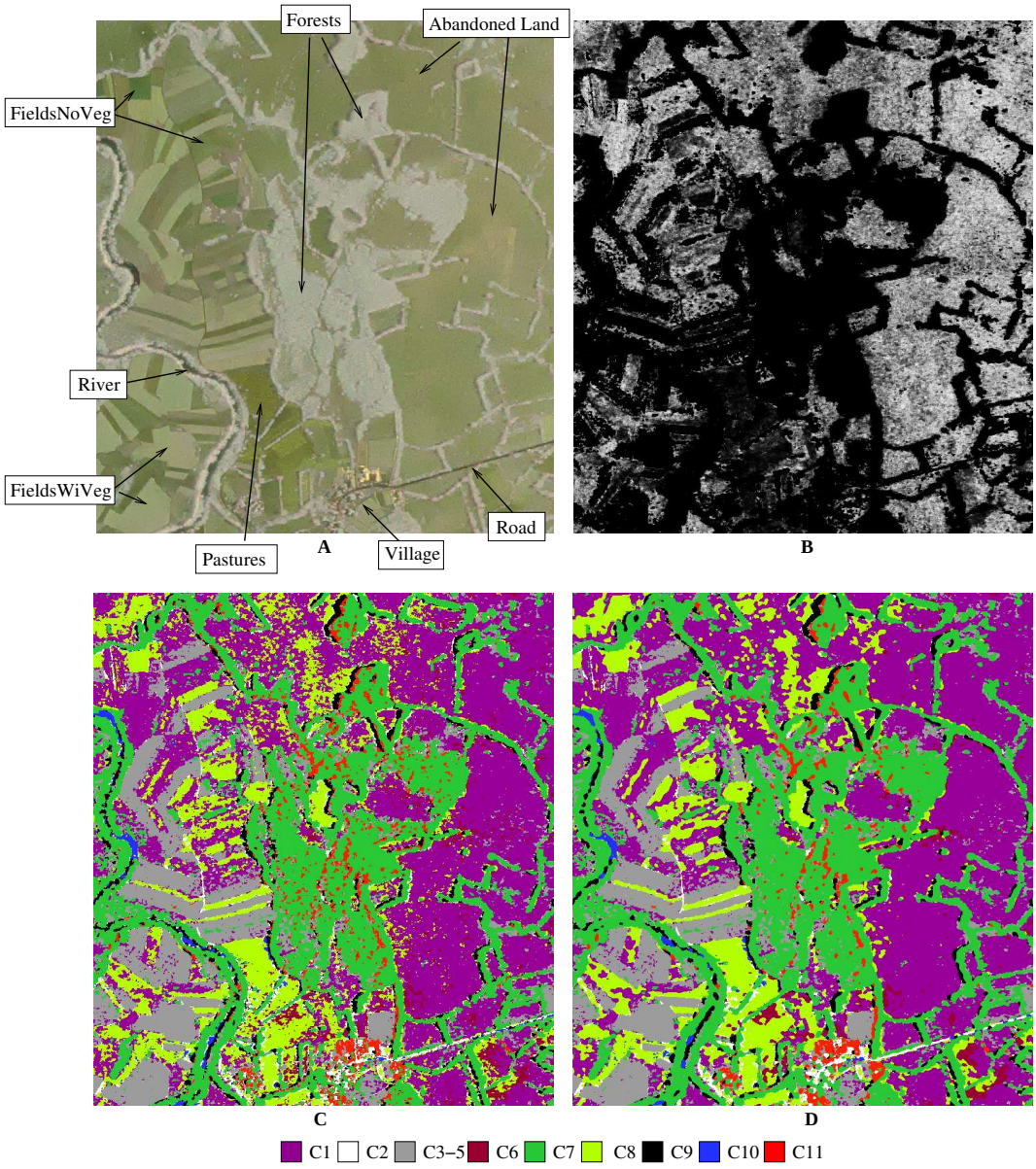

Figure 2. Results of the method: A: part of the speckle reduced polarimetric L-band image (R:HH, G:HV, B:VV) ©DLR, B: "detection image" for abandoned land, C: classification results (HM), D: Spatially regularized classification results (HM + SBR in 10×10 windows).

to the complement of the probability of false alarms. In fig. 3 UA is plotted against PA for the different classes. For each class, the figure shows the results for the three proposed classification methods and for the spatially regularized results of the HM method. As a comparison, the results obtained by the maximum likelihood (ML) classifier are also shown. The ML classifier results were obtained using the MultiSpec© package that is freely available at Purdue University. The figure provides a condensed way of presenting and comparing classification results. The best results are those with a high PA and UA, i.e.

corresponding to points in the upper right corner of the figure. The figure shows that for most classes the results obtained by MNLR and HM are better than those of ML. MNLR and HM are better than LR except for the classes "FieldsNoVeg" and "Residential". Closer inspection of the confusion matrices shows that fields without vegetation is heavily confused with Pastures. What is gained by LR in "FieldsNoVeg" equals the loss in "Pastures". The regularization by majority voting slightly improves the results of the HM method. The new regularization improves results for all classes even further except for the class "Forests" where PA is improved at the expense of UA. The relatively low value for the UA for "Residential Areas" is due to the fact that these regions are not homogeneous for a SAR system. The residential areas indeed include buildings, with double bounce reflectors and shadow areas as well as empty spaces between the buildings that can contain vegetation or asphalted surfaces.

Conf. Matrix		Classification Results									PA
		C1	C2	C3-5	C6	C7	C8	C9	C10	C11	(%)
V	C1	40715	73	1278	4060	374	15017	96	103	171	66
a	C2	4	612	74	2	184	77	55	70	259	46
l	C3-5	7350	51	23424	5	4451	3423	95	117	1788	58
i	C6	2280	528	588	398	5245	9275	27	246	1059	2
d	C7	54	26	133	0	16949	38	104	178	410	95
.	C8	523	50	109	5445	3	11177	47	51	0	64
S	C9	30	16	308	11	1188	71	4242	201	402	66
e	C10	2	40	25	1	293	5	302	2690	0	80
t	C11	0	236	232	36	1852	2	210	0	2601	50
UA(%)		80	38	90	4	56	29	82	74	39	

Table 3
Confusion matrix of final the result of HM+SBR and UA's and PA's

6 Conclusions

This paper presents a new method for supervised classification of multi-channel SAR images. The approach is feature based. The method allows us to take into account various types of features. In particular, radiometric, polarimetric, interferometric and spatial information were used as input features. These features are combined using logistic regression (LR), multinomial logistic regression (MNLR) and a hierarchical combination of both (HM). Both LR and

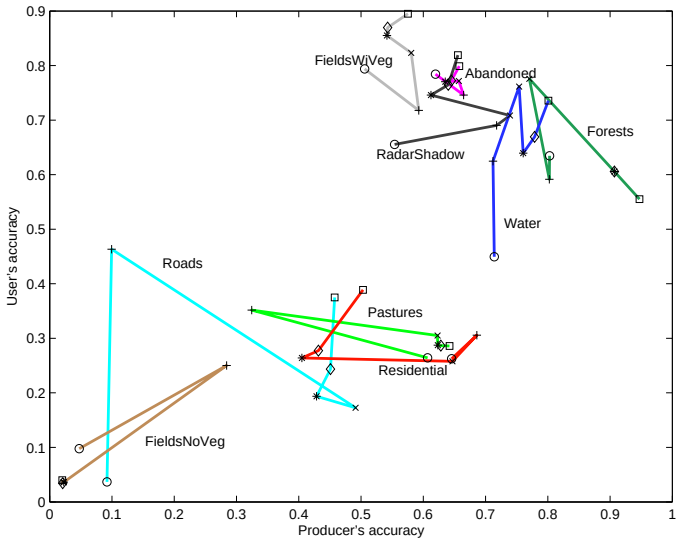

Figure 3. Results of different classification methods: UA vs. PA for the different classes. Legend: o ML, $+$ LR, $\times$ MNLR, $*$ HM, $\diamond$ HM with 3×3 MVR, $\square$ HM with 10×10 SBR

MNLR combine feature selection with the search for the classification function. A new spatial regularization method is also proposed. The proposed classification method is applied in a project on humanitarian demining where extensive ground-truth has been acquired for both learning and validation. The results are validated using statistical measurements on the obtained confusion matrix. Results are compared with a maximum likelihood (ML) classifier. For most classes MNLR and HM give the best results, which are better than those obtained by ML. The large land-cover classes are mostly correctly classified. An exception is "fields without vegetation" and "pastures" which are heavily confused by all methods. The input features do not contain information that allows to distinguish these two classes. Residential areas, which mainly consist of isolated agricultural dwellings in this scene, present problems because of their inhomogeneous character. The new spatial regularization method improves results significantly for most classes.

Acknowledgments

The presented research is the result of a collaboration between several projects: a Belgian Defense project (F00/07) on "Semi-automatic interpretation of SAR images"; ASARTECH: "Advanced SAR Technologies", funded by the Belgian Federal Science Policy (project nr. SR/00/04) and SMART: "Space and airborne Mined Area Reduction Tools", funded by the European Commission (project nr. IST-2000-25044). The results of the polarimetric decomposition as well as the interferometric coherences were provided by M. Keller of the

German Aerospace Agency (DLR). All images for the project were provided by the DLR.

References

V. Alberga, *Comparison of polarimetric methods in image classification and SAR interferometry applications*. PhD thesis, Fakultät für Elektrotechnik und Informationstecknik der Technischen Universität Chemnitz, Dresden, Jul 2003.

D. Borghys, A. Pizurica, C. Perneel, and W. Philips, "Combining multi-variate statistics and speckle reduction for line detection in multi-channel sar images," in *Proc. SPIE Vol. 5236, p. 93-104, SAR Image Analysis, Modeling, and Techniques VI; Francesco Posa; Ed.*, Sept 2003.

D. Borghys, C. Perneel, M. Keller, A. Pizurica, and W. Philips, "Supervised feature-based classification of multi-channel sar images using logistic regression," in *EUSAR 04*, (Ulm), May 2004.

D. Borghys, Y. Yvinec, C. Perneel, A. Pizurica, and W. Philips, "Hierarchical supervised classification of multi-channel sar images," in *3rd Int. Workshop on Pat. Recog. in Remote Sensing; Kingston-Upon-Thames*, Aug 2004.

S. Cloude and E. Pottier, "A review of target decomposition theorems in radar polarimetry," *IEEE-GRS*, vol. 34, p. 498, Mar 1996.

S. Cloude and E. Pottier, "An entropy based classification scheme for land applications of polarimetric sar," *IEEE-GRS*, vol. 35, pp. 68–78, Jan 1997.

M. Hellmann, *Classification of Fully Polarimetric SAR-Data for Cartographic Applications*. PhD thesis, Fakultät Elektrotechnik der Technischen Universität Dresden, Dresden, June 2000.

D. Hosmer and S. Lemeshow, *Applied Logistic Regression (2nd Edition)*. John Wiley and Sons, 2000.

J. Lee, M. Grunes, T. Ainsworth, L. Du, D. Schuler, and S. Cloude, "Unsupervised classification using polarimetric decomposition and the complex wishart classifier," *IEEE-GRS*, vol. 37, pp. 2249–2257, Sept 1999.

J. Lee, M. Grunes, and G. de Grandi, "Polarimetric sar speckle filtering and its implication for classification," *IEEE GRS*, vol. 37, pp. 2363–2373, Sept 1999.

A. Pizurica, W. Philips, I. Lemahieu, and M. Acheroy, "Despeckling sar images using wavelets and a new class of adaptive shrinkage estimators," in *Proc. IEEE Conf. on Image Proc. (ICIP)*, (Thessaloniki, Greece), Oct 2001.

A. Rodriguez, D.G. Corr, E. Pottier, L. Ferro-Famil, D. Hoekman, "Land Cover Classification using Polarimetric SAR Data", in *Proc. PolInSAR Conference*, (ESA-ESRIN, Frascati), Jan 2003.